Heating Performance Analysis of a Geothermal Heat Pump Working with Different Zeotropic and Azeotropic Mixtures

Robert Bedoić*1, *Veljko Filipan*2

1Faculty of Chemical Engineering and Technology, University of Zagreb, Savska cesta 16, Zagreb, Croatia
e-mail: rbedoic@fkit.hr
2Faculty of Chemical Engineering and Technology, University of Zagreb, Savska cesta 16, Zagreb, Croatia
e-mail: vfilipan@fkit.hr

ABSTRACT

The aim of the paper is to examine the possibility of application of the spreadsheet calculator and Reference Fluid Thermodynamic and Transport Properties database to a thermodynamic process. The heating process of a real soil-to-water heat pump, including heat transfer in the borehole heat exchanger has been analysed. How the changes of condensing temperature, at constant evaporating temperature, influence the following: heating capacity, compressor effective power, heat supplied to evaporator, compression discharge temperature and coefficient of performance, are investigated. Also, the energy characteristics of a heat pump using different refrigerants for the same heating capacity and the same temperature regime are compared. The following refrigerants are considered: two zeotropic mixtures, R407C and R409A, a mixture with some zeotropic characteristics, R410A, and an azeotropic mixture, R507A.

KEYWORDS

Heat pump, Reference fluid thermodynamic and transport properties database, Azeotropic and zeotropic mixtures.

INTRODUCTION

The use of zeotropic and azeotropic mixtures and their influence on the energy performance of a Geothermal soil-to-water Heat Pump (GHP) is examined in a previous paper [1]. There the influence of changes in evaporating temperature, at constant condensing temperature, on the energy performance such as: specific heat supplied to evaporator, specific heating capacity, specific compressor effective work, compression discharge temperature, and the Coefficient Of Performance (COP) was presented. Specific heating capacity and specific compressor effective work decrease as the evaporating temperature increases. At the same time specific heat supplied to evaporator increases. Finally, the COP values increase as the evaporating temperature increases. In this work, how the changes in condensing temperature, at constant evaporating temperature, influence the energy performance of the same GHP working with the same refrigerants, will be examined. R407C and R410A are selected as most commonly used refrigerants in different heat pump types [2]. Two other refrigerants that are not

---

* Corresponding author

prohibited, even though they are not used commonly, are selected for comparison. Synthetic refrigerants are widely used in Heating, Ventilation, and Air Conditioning (HVAC) systems, but according to Hydrofluorocarbon (HFC) Phase-Down Regulation, until 2030 almost 80% of HFCs should be replaced by some more environment-friendly refrigerants [3]. As possible replacement, hydrocarbons, ammonia and carbon dioxide are imposed [4]. In paper [5] the application of hydrocarbons as natural refrigerants for heat pump water heating is studied. R290 and R600a are considered as possible substitutes for R134a.

Use of soil as a heat source for a GHP that works in both heating and cooling mode is presented in [6]. Therein, experimental data are given for measured temperatures through the depth of the Borehole Heat Exchanger (BHE), at the beginning of operation and after a certain time of GHP operation. Thermo-physical properties of the ground for use in Geothermal Heat Pump (GHP) are investigated in [7]. Research covers both laboratory and field tests (thermal response test). Liu *et al.* [8] studied the use of two sources of heat, air and water, for heat pump in the heating mode. The impact of the heat source combination and outdoor temperature on the heating capacity and COP of the system is presented. Al-Hinti *et al.* [9] present measurements of climatic conditions and distribution of temperature at various depths of ground in order to investigate possible installation of GHP with horizontal heat exchangers. They also present a model of the soil temperature distribution as a function of time and depth. Bandos *et al.* [10] applied the line-source model for borehole heat exchangers and studied the effect of vertical temperature variations. Application of line source model for simulating near surface effects on borehole heat exchangers is studied in [11]. Authors presented the variation of temperature per depth of borehole using semi-analytical model and numerical model. Marcotte and Pasquier studied the application of numerical and line source model to describe the impact of operation time on temperature of fluid in borehole heat exchanger [12]. They also investigated the effect of following thermal parameters: ground thermal conductivity, ground thermal capacity and borehole thermal resistance on temperature of fluid in borehole heat exchanger in time. Chargui *et al.* [13] examined the mathematical simulation using TRNSYS software in a study of GHP in heating mode. They studied application of carbon dioxide as a refrigerant in a trans-critical cycle. Furthermore, [14] presents theoretical study of heat pump system for a high-temperature application composed of carbon dioxide trans-critical cycle and R152a subcritical cycle. The application of azeotropic mixtures as refrigerants for high temperature water source heat pump is analysed in [15]. Zeotropic (non-azeotropic) mixtures are also analysed as a possible replacement for allowed refrigerants in a heat pump [16]. Lv *et al.* [17] studied the application of zeotropic mixture composed of R32 and R290 in solar-assisted auto-cascade heat pump cycle. They examined the impact of temperature change in condenser and evaporator on COP values. In [18], the impact of variation of mass concentration in binary zeotropic mixture [R32/R1234ze(E)] on the energy performance of air-source heat pump is presented. The influence of pressure on the temperature glide of zeotropic and azeotropic mixtures is shown in [19] where the results are obtained by using a thermodynamic database for real fluids Reference Fluid Thermodynamic and Transport Properties (REFPROP) Version 8.0.

For the analysis in this paper, a newer Version 9.0 of the same thermodynamic database REFPROP is used. Also MS Office Excel spreadsheet is used for calculations in the first part of the paper where the influence of changes in condensing temperature, at constant evaporating temperature, on the energy performance of a GHP, and the energy characteristics of a GHP for the listed mixtures and same temperature conditions are analysed.

The second analysis here includes heat transfer from the ground to the refrigerant in a BHE. Using the analytical equations of one-dimensional approach [20], the ground

temperature change during the time of GHP operation, and also the influence of this temperature change on the energy characteristics of a GHP are examined.

MATERIALS AND METHODS

This section provides characteristics of chosen refrigerants using the REFPROP 9.0 database. Mathematical expressions used for calculation of energy performance and heat transfer in a BHE are also presented.

The characteristics of refrigerants

Refrigerants used in analysis are two zeotropic mixtures, R407C and R409A, a nearly zeotropic mixture, R410A and azeotropic mixture R507A. In order to examine the possibility of their application in the GHP, Table 1 contains their chemical composition (mass fraction) and Table 2 shows their critical parameters.

Table 1. The chemical composition and molar masses of refrigerants

Analyzed refrigerant	composition in mass [%]						M [kg kmol^{-1}]
	R22	R32	R124	R125	R134a	R142b	
R407C	23	-	-	25	52	-	86.204
R409A	60	-	25	-	-	15	97.433
R410A	-	50	-	50	-	-	72.585
R507A	-	-	-	50	50	-	98.859

The mixtures shown in Table 1 do not contain any of the prohibited Chlorofluorocarbons (CFC).

Table 2. The parameters of refrigerants

Analyzed refrigerant	Critical parameters		
	p [bar]	T [K]	V [m^3/kg]
R407C	46.293	359.18	0.0020653
R409A	46.986	382.41	0.0019649
R410A	49.019	344.50	0.0021761
R507A	37.050	343.77	0.0020376

Parameters from Table 2 show that analyzed zeotropic mixtures have higher critical temperature in comparison to the other two refrigerants. Additionally, Figure 1 shows the position and shape of the saturation curves on a *T-s* diagram for the analysed refrigerants. The REFPROP 9.0 database is used for the construction of the diagram.
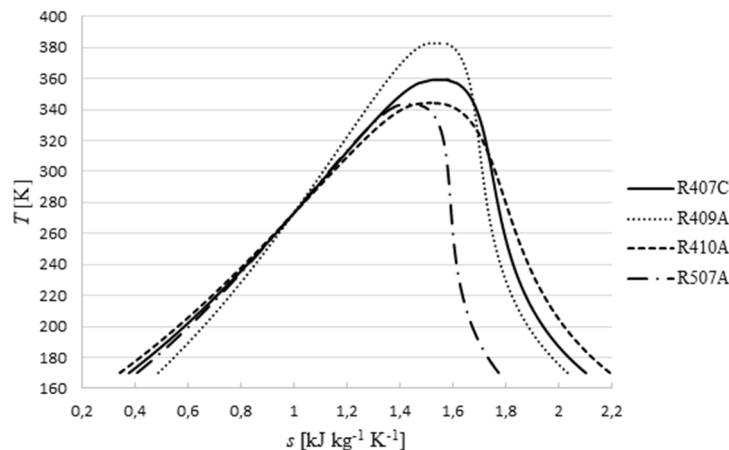

Figure 1. Saturation curves of the analysed refrigerants in the *T-s* diagram

The maximum condensing temperature is limited by the critical temperature of the refrigerant in the subcritical heat pump cycle. Therefore, the analyzed zeotropic mixtures can be used for higher temperature application compared to azeotropic mixture (cca 15 °C or 40 °C).

Thermodynamic analysis of a heat pump cycle

Specific states of refrigerant in a heat pump cycle and proper description are given in Table 3.

Table 3. The specific states of refrigerant in a heat pump cycle

Thermodynamic state	Description
1˝	Saturated vapour at evaporating pressure
1	Superheated vapour at compressor inlet
2s	Superheated vapour at the end of isentropic compression (hypothetical)
2	Superheated vapour at the end of compression with isentropic efficiency, $\eta < 1$
3˝	Saturated vapour at condensing pressure
3´	Boiling liquid at condensing pressure
4	Subcooled hot liquid at condensing pressure
5	Liquid and vapour mixture at the exit of throttle valve

To describe the thermodynamic performance of the analysed cycle some assumptions were used:

- The whole system is assumed to be in thermodynamic equilibrium;
- Pressure loss and heat loss in heat exchangers are neglected;
- Isentropic efficiency, $\eta < 1$, is introduced for the compression process:

$$\eta = \frac{w_s}{w} = \frac{h_1 - h_{2s}}{h_1 - h_2} \tag{1}$$

where h_1 represents the enthalpy value of the refrigerant at compressor inlet, h_{2s} is the enthalpy of the refrigerant at the end of hypothetical isentropic compression and h_2 is the enthalpy of the refrigerant at the end of compression with isentropic efficiency, $\eta < 1$.

Compression discharge temperature, ϑ_2 at condensation pressure and enthalpy h_2 can be determined after the enthalpy h_2 is calculated as:

$$h_2 = h_1 - \frac{h_1 - h_{2s}}{\eta} \tag{2}$$

Specific heating capacity can be calculated as:

$$q_c = h_4 - h_2 \tag{3}$$

where h_4 represents the enthalpy of subcooled refrigerant at condensation pressure.

Specific heat supplied to evaporator can be calculated as:

$$q_e = h_1 - h_5 \tag{4}$$

where h_5 represents the enthalpy of refrigerant at the entrance to evaporator (the same as enthalpy h_4).

As the mass flow rate of refrigerant is constant in the cycle, heat flow rates in heat exchangers and compressor effective power can be calculated as:

$$\Phi_e = q_e \cdot \dot{m} \tag{5}$$

$$\Phi_c = q_c \cdot \dot{m} \tag{6}$$

$$P = w \cdot \dot{m} \tag{7}$$

COP is defined as:

$$COP = \frac{q_c}{w} = \frac{\Phi_c}{P} \tag{8}$$

The number of the compressor cycles per unit time ($\dot{n}$) is a function of mass flow rate ($\dot{m}$), specific volume of the refrigerant at the entrance to compressor (v_1) and compressor cylinder volume (V) and can be defined as:

$$\dot{n} = \frac{v_1 \cdot \dot{m}}{V} \tag{9}$$

Thermodynamic analysis of heat transfer in a Borehole Heat Exchanger

In order to describe heat transfer in the BHE, 1-D approach is used according to [20]. Due to high ratio of length to radius of borehole, heat transfer in the axial direction is neglected. The partial differential equation used for the description of conductive heat transfer in the radial direction is:

$$\frac{\partial T}{\partial t} = a \left(\frac{\partial^2 T}{\partial r^2} + \frac{1}{r} \frac{\partial T}{\partial r} \right) \tag{10}$$

The thermal diffusivity of the ground, a, is defined by the equation:

$$a = \frac{\lambda}{C} \tag{11}$$

where λ isthermal conductivity and C is the volumetric heat capacity of the ground.

The heat transfer rate, $\dot{q}$, is defined by the eq. (12):

$$\dot{q} = -2\pi\lambda r_0 \left(\frac{\partial T}{\partial t} \right) \tag{12}$$

along with initial condition $T(r,0) = T_0$. Eq. (10) and (12) can be solved in several ways, and one solution is adopted:

$$T(r,t) = T_0 + \frac{\dot{q}}{4\lambda\pi} E_i \left(\frac{r^2}{4at} \right) \tag{13}$$

Figure 2 shows the cross-section of BHE, and the position of grout and ground [21].
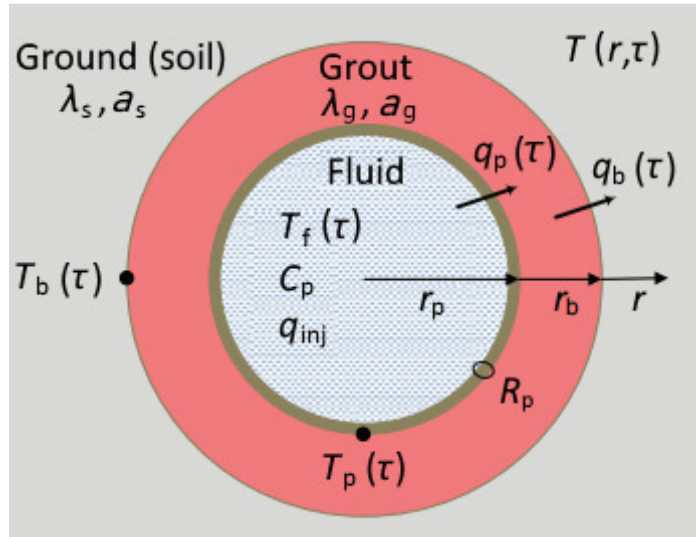
Figure 2. Cross-section of BHE [21]

Carslaw-Jaeger [20] suggested the solution to exponential integral function (E_i), according to approximation defined by eq. [20]:

$$E_i\left(\frac{r^2}{4at}\right) \cong \ln\left(\frac{4at}{r^2}\right) - \gamma \tag{14}$$

where γ is Euler's constant with an approximate value of 0.5772. When the approximation is inserted in eq. (13), the new equation (infinite line source) is introduced:

$$T(r,t) - T_0 = \frac{\dot{q}}{4\lambda\pi}\left[\ln\left(\frac{4at}{r^2}\right) - \gamma\right] \tag{15}$$

Use of eq. (15) is possible only with constant heat transfer rate. Deficiency of that approach to heat transfer is in the impossibility of the model to predict the temperature for:

$$t \le \frac{r^2}{4a} \tag{16}$$

It is convenient to introduce the dimensionless radius R which is defined by the eq. (17):

$$R = \frac{r}{r_0} \tag{17}$$

Position R is always greater than 1. For the defined constant R, the temperature of ground is observed only as a function of time:

$$T(t) - T_0 = \frac{\dot{q}}{4\lambda\pi}\left[\ln\left(\frac{4at}{R^2 r_0^2}\right) - \gamma\right] \tag{18}$$

During the time of GHP operation ($t > 0$) in the heating mode, heat is taken from the ground and transferred to BHE. Therefore, $\dot{q}$ is considered negative and the temperatures follow relation $T(t) < T_0$ or $\vartheta(t) < \vartheta_0$ when expressed in Celsius scale:

$$\vartheta(t) - \vartheta_0 = \frac{\dot{q}}{4\lambda\pi}\left[\ln\left(\frac{4at}{R^2 r_0^2}\right) - \gamma\right] \tag{19}$$

Heat transferred from the ground to BHE is defined as:

$$\Phi_g = \frac{1}{R_{BHE}} \cdot L \cdot \Delta\vartheta_t \tag{20}$$

where L presents the length of vertical borehole. R_{BHE} is the borehole thermal resistance, the measured data from thermal response test. The assumption is that R_{BHE} remains constant through the borehole depth and it is taken from literature. The driving force $\Delta\vartheta_t$ is defined by:

$$\Delta\vartheta_t = \frac{\left[\vartheta(t_i) - \vartheta_e\right] + \left[\vartheta(t_{i-1}) - \vartheta_e\right]}{2} \tag{21}$$

where $\vartheta(t_i)$ presents the temperature of ground in time t_i, $\vartheta(t_{i-1})$ presents the temperature of ground before time increment (Δt) in a previous time t_{i-1} and ϑ_e presents the evaporating temperature of refrigerant in evaporator. Constant pressure in evaporator is assumed, so the temperature of evaporation does not change. The assumption is that the heat taken from ground is directly transferred to refrigerant in evaporator. BHE is assumed to be the evaporator of refrigerant and therefore the eq. (21) is used. In a real system, circulating fluid inside BHE takes heat from ground and transfers it to refrigerant in evaporator.

RESULTS & DISCUSSION

In this section results obtained using the observed methods are given. They are shown in diagrams with appropriate axis notation, units and legends.

Thermodynamic process in the Geothermal Heat Pump

In order to investigate the behaviour of refrigerants at different temperature, the evaporating temperature/dew point ($\vartheta_{1''}$) is held constant (0 °C), and the condensing temperature/bubble point ($\vartheta_{3'}$) is changed from 40 °C to 60 °C.

All results are given for the superheating of saturated vapour in evaporator for 5 °C, and for liquid subcooling in condenser for 5 °C. Isentropic efficiency of the compressor is set at 60%. Volume of the compressor cylinder is set to 2 dm^3. For all analysed temperature regimes, the heating capacity is set to $\Phi_c = 20$ kW.

The thermodynamic process in the examined GHP with application of R410A is displayed in the T, h diagram in Figure 3 for illustration. The diagram is displayed for the condensation temperature of 50 °C.

On Figure 3, it can be seen that the compression discharge temperature (T_2) in a process with isentropic efficiency, $\eta < 1$ is higher than in the process with isentropic compression (T_{2s}). It results in higher specific heating capacity, but also increases specific compressor effective work. In saturation area it can be seen that mixture R410A shows no temperature glide that is a characteristic of azeotropic mixtures. In this case, calculation of states near critical point is avoided because REFPROP gives somewhat doubtful results.
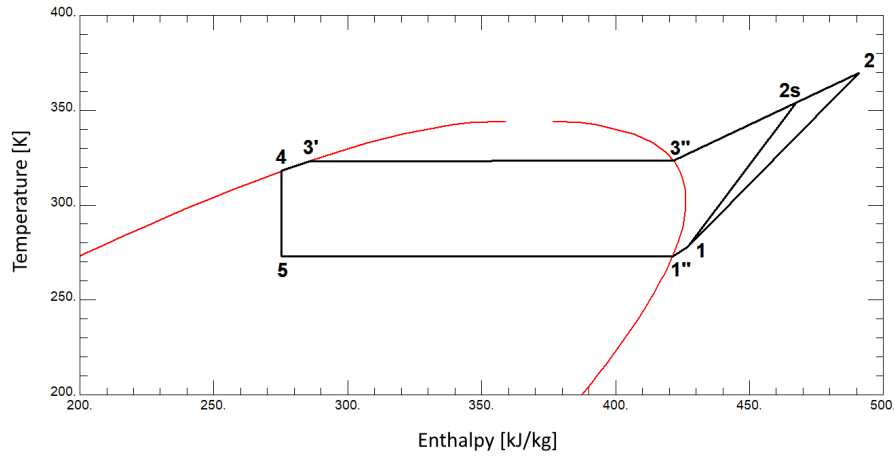
Figure 3. *T, h* diagram of the analysed thermodynamic process with R410A

Figure 4 shows the impact of condensing temperature on the specific heat supplied to evaporator (q_e, dark blue lines) and specific heating capacity (q_c, red lines) for analysed refrigerants. Figure 5 shows the impact of condensing temperature on the COP values for analysed refrigerants.
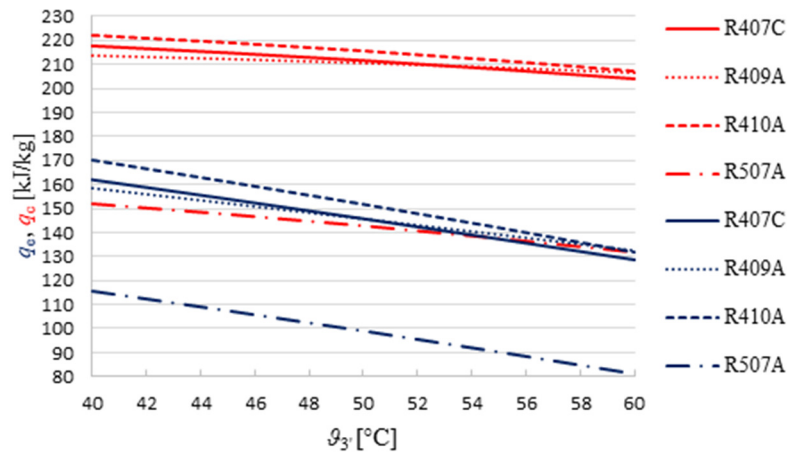

Figure 4. Impact of condensing temperature change ($\vartheta_{3'}$) on specific heat supplied to evaporator (q_e) and specific heating capacity (q_c) for analysed refrigerants
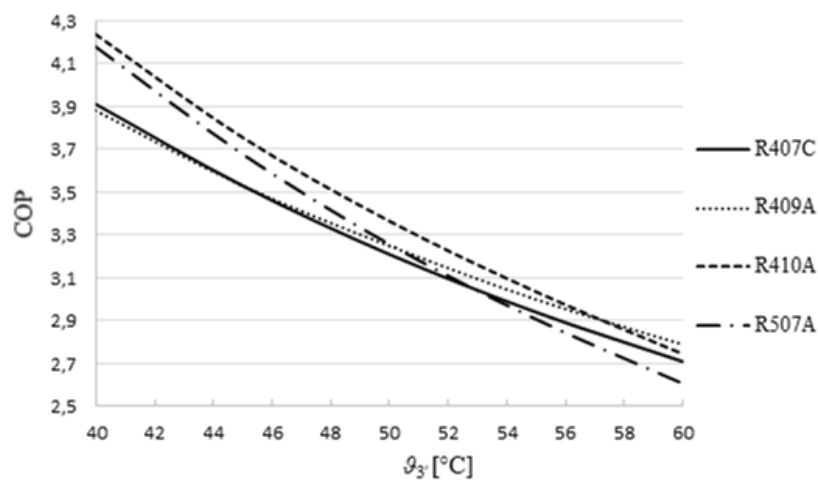

Figure 5. Impact of condensing temperature change ($\vartheta_{3'}$) on the COP values for analysed refrigerants

It can be seen from Figure 4 that with the increase of $\vartheta_{3'}$ the specific heat supplied to evaporator (q_e) and specific heating capacity (q_c) decrease while the specific compressor effective work (w) increases. As a result, the values of COP significantly decrease as shown on Figure 5. R410A and R507A show higher values of COP at lower condensing temperature compared to other two refrigerants. COP curve for R507A has the steepest fall and eventually it reaches the lowest COP value at the temperature of 60 °C. Comparing the results obtained for the same temperature regime, but for different refrigerants, it can be seen that the specific heat supplied to evaporator (q_e) and specific heating capacity (q_c) of azeotropic mixture (R507A) is significantly lower than for other refrigerants.

Figure 6 presents the impact of condensing temperature on heat supplied to evaporator (Φ_e, dark blue lines) and compressor effective power (P, black lines).
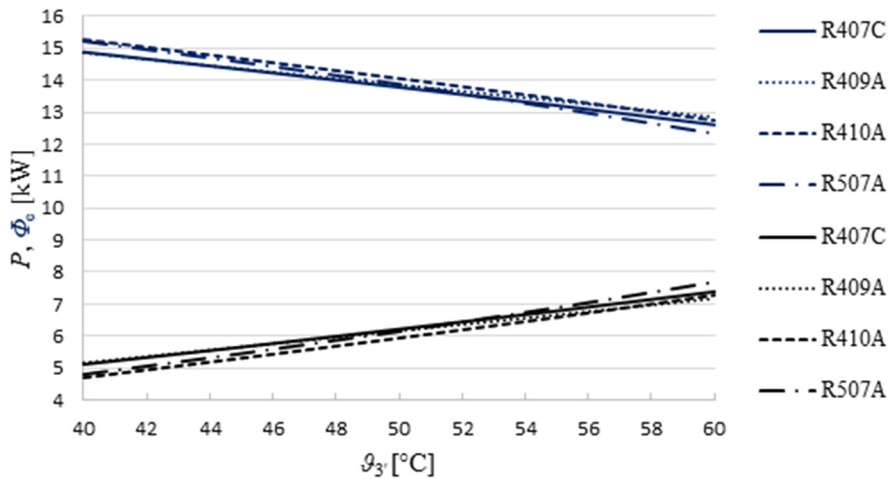

Figure 6. Impact of condensing temperature change ($\vartheta_{3'}$) on the heat supplied to evaporator (Φ_e) and compressor effective power (P) for analysed refrigerants

The calculated heat supplied to evaporator (Φ_e) decreases and compressor effective power (P) increases with the increase of $\vartheta_{3'}$ to provide the constant heating capacity ($\Phi_c = 20$ kW). The significant increasing of compressor effective power with condensing temperature appears to be for R507A, from 4.79 kW for $\vartheta_{3'} = 40$ °C to 7.67 kW for $\vartheta_{3'} = 60$ °C. R410A is shown to have the highest values of heat supplied to evaporator (15.28 kW for $\vartheta_{3'} = 40$ °C and 12.74 kW for $\vartheta_{3'} = 60$ °C).

Table 4 presents specific volume of refrigerants at the entrance to compressor for calculation of number of cycles per unit time.

Table 4. The specific volume at the entrance to the compressor (v_1) for the examined refrigerants

Analysed refrigerant	v_1 [m^{3}kg^{-1}]
R407C	0.0522
R409A	0.0767
R410A	0.0339
R507A	0.0320

Figure 7 presents the impact of condensing temperature to mass flow rate ($\dot{m}$, light blue curves) and number of cycles per unit time ($\dot{n}$, green curves).

The calculated mass flow rate of the refrigerant ($\dot{m}$) and the number of compressor cycles per unit time ($\dot{n}$), are slightly increasing with the increase of $\vartheta_{3'}$ as to obtain the

constant heating capacity (Φ_c = 20 kW). From Table 4 it can be seen that the specific volumes (v_1) of zeotropic mixtures (R407C and R409A) are significantly higher in comparison with other refrigerants (R410A andR507A). R409A has the highest v_1 and so the compressor should have the highest number of cycles (about 220 c. per min.) for obtaining the same constant heating capacity (Φ_c). R507A has the lowest v_1 but its compressor cycles are not the lowest because of the highest mass flow rate of this refrigerant ($\dot{n}$ is about 135 c. per min.). The lowest mass flow rate (about 0.095 kg per sec.) and low specific volume (0.034 m^3 per kg) result with the lowest compressor cycles (about 94 c. per min.) for R410A.
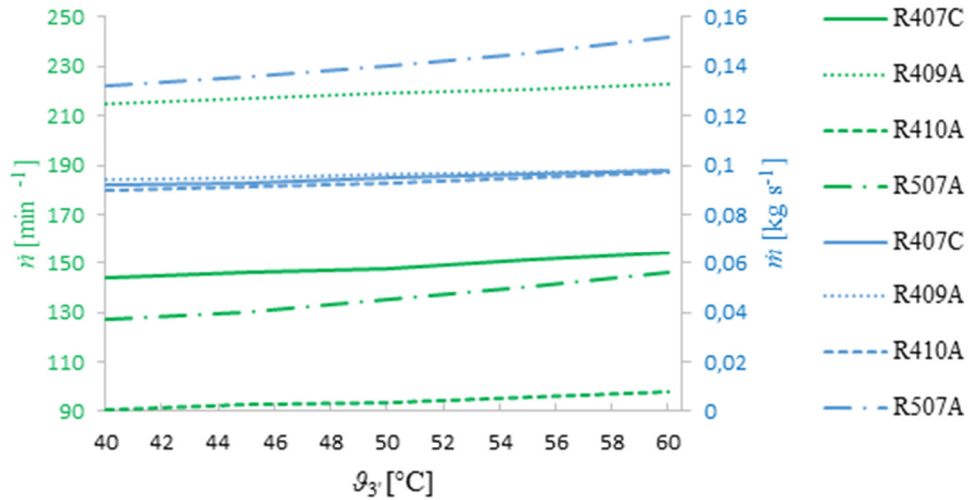

Figure 7. Impact of condensing temperature change ($\vartheta_{3'}$) on the mass flow rate ($\dot{m}$) and number of cycles per unit time ($\dot{n}$) for analysed refrigerants

Figure 8 presents the impact of condensing temperature to compression discharge temperature (ϑ_2, violet lines) and bubble point temperature ($\vartheta_{3''}$, red lines).
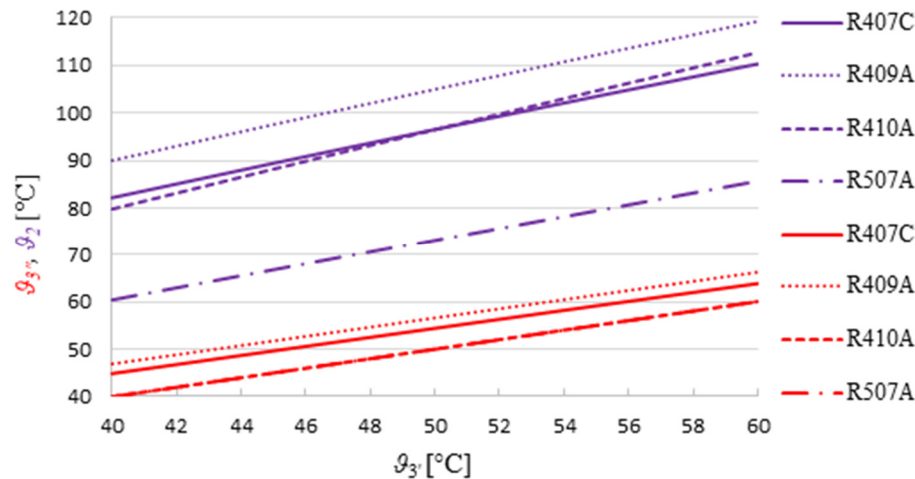

Figure 8. Impact of condensing temperature change ($\vartheta_{3'}$) on the compression discharge temperature (ϑ_2) and bubble point temperature ($\vartheta_{3''}$) for analysed refrigerants

Compression discharge temperature (ϑ_2) is also increasing with the increase of temperature $\vartheta_{3'}$. All these show that efficiency of GHP decreases when they are used for high-temperature applications. Comparing the compression discharge temperatures (ϑ_2) for different refrigerants it can be seen that the lowest values (between 61 °C and 86 °C)

are obtained for the azeotropic mixture (R507A). Much higher values are calculated for zeotropic mixtures (R407C and R409A) and R410A, with the highest values for R409A (between 90 °C and 119 °C). It is partially caused by the temperature glide at the constant evaporating and condensing pressures which for zeotropic mixture can be up to 7 °C. High COP and low compression discharge temperatures could make the azeotropic mixtures as a good choice for the GHP refrigerants.

Heat transfer in the Borehole Heat Exchanger

In order to study the heat transfer between BHE and refrigerant the following data are used: the evaporating temperature of refrigerant is constant and equal to $\vartheta_e = 0$ °C, starting temperature of ground is $\vartheta_0 = 15$ °C, radius is $r_0 = 0.030$ m, position is defined by $R = 1$ and the length of borehole L is 100 m. The assumption is that starting temperature of ground is the same through the length of borehole. Temperatures during BHE operation are calculated with time increment $\Delta t = 0.02$ h. To describe impact of the time of GHP operation on the heat transferred, the following average values along borehole length are used [22]: R_{BHE} is assumed to be 0.091 K mW^{-1}, $\lambda = 1.80$ W m^{-1}K^{-1} and $C = 2,180$ kJ m^{-3}K^{-1}. In [23] it is stated that values for heat flow rate in a BHE appeared to be between 20 and 50 W m^{-1}. In this calculation negative values of heat flow rates are used due to heat transfer from ground to refrigerant.

Figure 9 shows the heat removed from the ground (Φ_g) vs. time of operation (t) for some studied heat flow rates ($\dot{q}$).
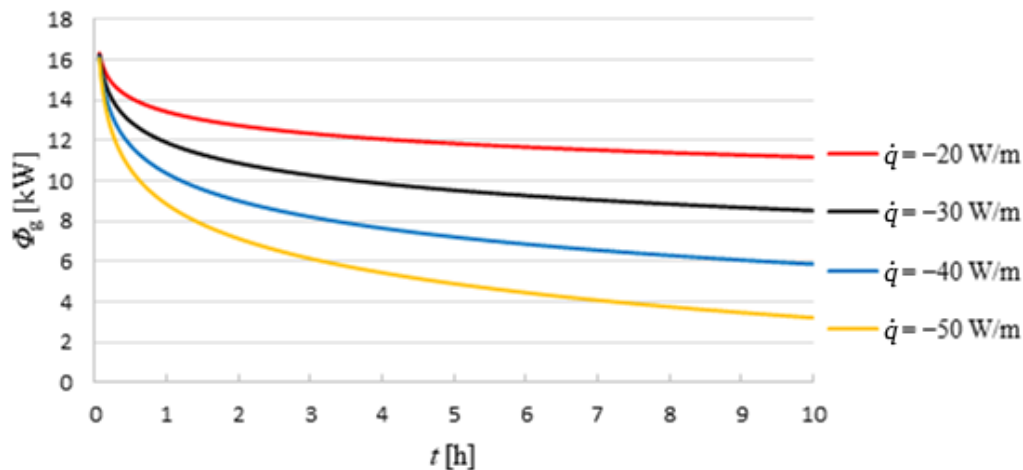

Figure 9. Impact of BHE time of operation (t) and heat flow rate ($\dot{q}$) on the ground heat (Φ_g)

Heat removed from the ground and at the same time supplied to evaporator decreases as the time of BHE operation increases. The higher the heat flow rate, the more heat is transferred from the ground to refrigerant. Calculation starts at 0.08 h according to limitation of model given by the eq. (16).

Furthermore, how the change in evaporating pressure (temperature) of the refrigerant affects the heat transfer between BHE and refrigerant was studied. The temperature vs. time dependence is given by the eq. (19). All parameters were used as in previous calculation. Initial temperature of the ground is $\vartheta_0 = 15$ °C and heat flow rate is assumed to be constant, $\dot{q} = -50$ W m^{-1}. Figure 10 shows impact of the evaporating temperature (ϑ_e) on the heat removed from the ground (Φ_g) for some different time of operation (t).

According to calculation and results presented in Figure 10, as the evaporating temperature of refrigerant increases, the heat taken from the ground and at the same time supplied to evaporator decreases. In study [1] it is presented that heat supplied to evaporator increases as the evaporating temperature increases. That relation is valid only

if there is an unlimited source of heat for refrigerant in evaporator. This study has also shown that ground is a very limited source of heat so it should be taken into account during the analysis of a GHP operation.
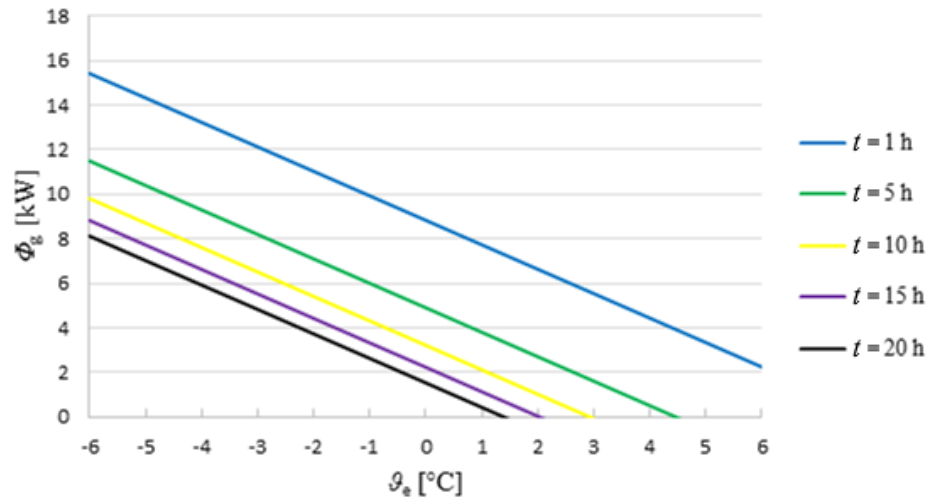

Figure 10. Impact of the change in refrigerant evaporating temperature (ϑ_e) on the heat removed from the ground (Φ_g) for different times of operation (t)

CONCLUSIONS

In the same temperature regime, azeotropic mixtures show lower values of specific heat supplied to evaporator and specific heating capacity and lower compression discharge temperature compared to zeotropic mixtures. From presented energy performance, R410A and R507C are assumed to be more appropriate refrigerants for use. R410A shows the greatest COP values and the lowest required compressor effective power for the same heating capacity. R507C shows also high COP and low compression discharge temperatures. Zeotropic mixtures show temperature glide in two-phase area that could result in lower required area for heat transfer.

Ground, as a heat source for GHP is very complex for analysis. In the present study the calculations were made using a simple 1D model of heat transfer in the BHE. The variation of temperature along the depth could not be taken into account, although this is a case in a real system as determined by experiments. Using the simplified 1D model the changes in temperature of ground during the GHP operation are calculated. The results show that ground is a limited source of heat due to its cooling with the time of GHP operation. Also, it is shown that rise in the evaporating temperature of the refrigerant decreases the driving force to the heat transfer and heat removed from the ground. Accuracy of this calculation should be tested by experimental data in order to make improvements and further development.

NOMENCLATURE

a	thermal diffusivity of the ground	$[\text{m}^2\text{s}^{-1}]$
C	volumetric heat capacity of the ground	$[\text{kJ m}^{-3}\text{K}^{-1}]$
h	enthalpy of refrigerant	$[\text{kJ kg}^{-1}]$
L	length of borehole	$[\text{m}]$
$\dot{m}$	mass flow rate	$[\text{kg s}^{-1}]$
$\dot{n}$	number of cycles per unit time	$[\text{min}^{-1}]$
P	compressor effective power	$[\text{kW}]$
q_c	specific heating capacity	$[\text{kJ kg}^{-1}]$
q_e	specific heat supplied to evaporator	$[\text{kJ kg}^{-1}]$

$\dot{q}$	heat transfer rate	[W m^{-1}]
r	radius	[m]
R	dimensionless radius	[m m^{-1}]
R_{BHE}	borehole thermal resistance	[K mW^{-1}]
t	time	[h]
T	thermodynamic temperature	[K]
w	specific compressor effective work	[kJ kg^{-1}]

Greek letters

η	compressor isentropic efficiency	[%]
ϑ	Celsius temperature	[°C]
λ	thermal conductivity of ground	[W m^{-1}K^{-1}]
Φ	heat flow rate	[kW]

Subscripts and superscripts

c	condensation
e	evaporation
g	ground
0	initial temperature of BHE, radius of borehole
s	isentropic
'	boiling liquid
"	saturated vapour

REFERENCES

1. Bedoić, R. and Filipan, V., The analysis of Heat transfer in a Compression Heat Pump working with different Zeotropic and Azeotropic Mixtures , 7th International Forum on Renewable Energy Sources Rovinj, 2016, http://www.em.com.hr/eipp/rad/1130, [Accessed: 09-March-2017]
2. European Commission, Heat Pumps – Technology and Environmental Impact, http://ec.europa.eu/environment/ecolabel/about_ecolabel/reports/hp_tech_env_impact_aug2005.pdf, [Accessed: 12-September-2013]
3. European Commission, EU Legislation to Control F-gases, https://ec.europa.eu/clima/policies/f-gas/legislation_en, [Accessed: 12-September-2013]
4. European Commission, Climate-friendly alternatives to HFCs and HCFCs, https://ec.europa.eu/clima/policies/f-gas/alternatives_en, [Accessed: 12-September-2013]
5. Nawaz, K., Shen, B., Elatar, A., Baxter, V. and Abdelaziz, O., R290 (propane) and R600a (isobutane) as Natural Refrigerants for Residential Heat Pump Water Heaters, *Applied Thermal Engineering*, Vol. 127, pp 870-883, 2017, https://doi.org/10.1016/j.applthermaleng.2017.08.080
6. Soldo, V., Boban, L. and Borović, S., Vertical distribution of Shallow Ground Thermal properties in different Geological Settings in Croatia, *Renewable Energy*, Vol. 99, pp 1202-1212, 2016, https://doi.org/10.1016/j.renene.2016.08.022
7. Luo, J., Rohn, J., Xiang, W., Bertermann, D. and Blum, P., A Review of Ground Investigations for Ground Source Heat Pump (GSHP) Systems, *Energy and Buildings*, Vol. 117, pp 160-175, 2016, https://doi.org/10.1016/j.enbuild.2016.02.038
8. Liu, X., Ni, L., Lau, S.-K. and Li, H., Performance analysis of a Multi-functional Heat Pump System in Heating Mode, *Applied Thermal Engineering*, Vol. 51, No. 1-2, pp 698-710, 2013, https://doi.org/10.1016/j.applthermaleng.2012.08.043
9. Al-Hinti, I., Al-Muhtady, A. and Al-Kouz, W., Measurement and modelling of the Ground Temperature Profile in Zarqa, Jordan for Geothermal Heat Pump Applications,

Applied Thermal Engineering, Vol. 123, pp 131-137, 2017, https://doi.org/10.1016/j.applthermaleng.2017.05.107

10. Bandos, V., T., Montero, Á., Fernández, E., Santander G. J. L., Isidroa, J. M., Pérez, J., Fernández de Córdobaa, J. P. and Urchueguía, F. J., Finite Line-source Model for Borehole Heat Exchangers: Effect of Vertical Temperature Variations, *Geothermics*, Vol. 38, No. 2, pp 263-270, 2009, https://doi.org/10.1016/j.geothermics.2009.01.003

11. Rivera, A. J., Blum, P. and Bayer, P., A Finite Line Source Model with Cauchy-type Top Boundary Conditions for Simulating near Surface Effects on Borehole Heat Exchangers, *Energy*, Vol. 98, pp 50-63, 2016, https://doi.org/10.1016/j.energy.2015.12.129

12. Marcotte, D. and Pasquier, P., On the estimation of Thermal Resistance in Borehole Thermal Conductivity Test, *Renewable Energy*, Vol. 33, No. 11, pp 2407-2415, 2008, https://doi.org/10.1016/j.renene.2008.01.021

13. Chargui, R., Sammouda, H. and Farhat, A., Geothermal Heat Pump in Heating Mode: Modeling and Simulation on TRNSYS, *International Journal of Refrigeration*, Vol. 35, No. 7, pp 1824-1832, 2012, https://doi.org/10.1016/j.ijrefrig.2012.06.002

14. Yang, W-w., Cao, X-q., He, Y-l. and Yan, F-y., Theoretical Study of a High-temperature Heat Pump System composed of a CO_2 Transcritical Heat Pump Cycle and a R152a Subcritical Heat Pump Cycle, *Applied Thermal Engineering*, Vol. 120, pp 228-238, 2017, https://doi.org/10.1016/j.applthermaleng.2017.03.098

15. Zhang, S., Wang, H. and Guo, T., Experimental investigation of moderately high Temperature Water Source Heat Pump with non-azeotropic Refrigerant Mixtures, *Applied Energy*, Vol. 87, No. 5, pp 1554-1561, 2010, https://doi.org/10.1016/j.apenergy.2009.11.001

16. Lee, Y., Kang, D. and Jung, D., Performance of Virtually non-flammable Azeotropic HFO1234yf/HFC134a Mixture for HFC134a Applications, *International Journal of Refrigeration*, Vol. 36, No. 4, pp 1203-1207, 2013, https://doi.org/10.1016/j.ijrefrig.2013.02.015

17. Lv, X., Yan, G. and Yu, J., Solar-assisted Auto-cascade Heat Pump Cycle with Zeotropic Mixture R32/R290 for Small Water Heaters, *Renewable Energy*, Vol. 76, pp 167-172, 2015, https://doi.org/10.1016/j.renene.2014.11.012

18. Cheng, Z., Baolong, W., Shi, W. and Li, X., Numerical research on R32/R1234ze(E) Air Source Heat Pump under Variable Mass Concentration, *International Journal of Refrigeration*, Vol. 82, pp 1-10, 2017, https://doi.org/10.1016/j.ijrefrig.2017.06.014

19. Sagia, Z. and Rakopoulos, C., Alternative Refrigerants for the Heat Pump of a Ground Source Heat Pump System, *Applied Thermal Engineering*, Vol. 100, pp 768-774, 2016, https://doi.org/10.1016/j.applthermaleng.2016.02.048

20. Al-Khoury, R., *Computational Modeling of Shallow Geothermal Systems*, CRC Press, Boca Raton, USA, 2011.

21. Javed, S. and Claesson, J., New analytical and numerical Solutions for the Short-term analysis of Vertical Ground Heat Exchangers, *ASHRAE Transactions*, Vol. 117, No. 1, pp 3-12, 2011.

22. Soldo, V., Borović, S., Lepoša, L. and Boban, L., Comparison of different Methods for Ground Thermal properties determination in a Clastic Sedimentary Environment, *Geothermics*, Vol. 61, pp 1-11, 2016, https://doi.org/10.1016/j.geothermics.2015.12.010

23. Svec, O. J., Goodrich, L. E. and Palmer, J. H. L., Heat transfer characteristics of In-ground Heat Exchangers, *Energy Research*, Vol. 5, pp 265-278, 1983, https://doi.org/10.1002/er.4440070307